Hfs of F^{19} in the Electron Paramagnetic Resonance of $MgF_2:Co^{++}$

H. M. GLADNEY
IBM Research Laboratory, San Jose, California
(Received 23 July 1965; revised manuscript received 23 August 1965)

The complex hyperfine structure of the X-band EPR spectra of Co^{++} as a dilute substitutional impurity in a single crystal of MgF_2 has been assigned. Where the x and z axes are taken along the bond direction of the two equivalent fluorine ions and along the crystalline c axis, respectively, the values of the spin-Hamiltonian tensors are: for the gyromagnetic ratio (6.0327, 2.2970, 4.2391) Mc/sec; for the cobalt hyperfine interaction, (637.1, 123.3, 210.0) Mc/sec; for the hfs of the two equivalent F^{19} nuclei along the [110] direction, (308, 59, 76) Mc/sec; for the four equivalent F^{19} nuclei in the [110] plane, (92, 76, 162, 49) Mc/sec. In the last case the final component is the off-diagonal yz contribution. First-order perturbation theory for the F^{19} superhyperfine structure predicts splittings independent of the cobalt nuclear-spin number. However, even though the F^{19} interactions are two orders of magnitude smaller than the Zeeman effect, for some magnetic-field orientations the observed splittings vary as much as 50% across the spectrum. The effect may be traced to fourth-order perturbations (squared in both the Co hyperfine and F^{19} hyperfine interaction) between nearly degenerate states. A set of computer programs to relate EPR spectra to spin-Hamiltonian parameters was essential to the analysis reported.

I. INTRODUCTION

LONG ago, Tinkham[1] observed the electron-paramagnetic-resonance spectrum of Co^{++} as a dilute substitutional impurity in ZnF_2, but did not complete the investigation because inadequate resolution made analysis of the very complex hyperfine structure too difficult. It is the purpose of this paper to show the analysis of the hyperfine spectra of Co^{++} in MgF_2, a similar low-symmetry environment, and to determine the parameters of the spin Hamiltonian for subsequent analysis of the electronic structure and chemical bonding.

EPR has long been considered one of the most useful tools for the experimental study of chemical bonding. Because the ground state of Co^{++} in an octahedral field is orbitally degenerate, both the electronic spin and the orbital motion contribute to the magnetic moment, so that the paramagnetic resonance spectrum of this species is of particular interest. It has been extensively studied both in cubic[2–4] and in lower symmetry[3–8] environments. Abragam and Pryce[9] have given a crystal-field interpretation of the gyromagnetic and Co-hyperfine tensors in axial symmetry. Tinkham has extended this theory to orthorhombic symmetry. However, as we have shown[10] in the case of Ti^{3+}, inferences about the extent of covalent bonding based on reductions of orbital angular momentum, of effective spin-orbit coupling and term separations over the values expected for free ions are tenuous at best, and possibly quite misleading.[11] Fortunately, more direct measures of electron sharing are available in the hyperfine interaction of nuclei remote from the ion nominally carrying the unpaired electron(s) responsible for a resonance spectrum. It may be argued from both experimental and theoretical considerations that some of the most promising physical systems for study are transition-metal cations as dilute substitutional impurities in diamagnetic fluoride lattices. The hyperfine interactions are very large. Single crystals of a number of fluorides are relatively easily available, are stable and characterized without difficulty. Although electron sharing is large enough to be easily observed, it is not so large that an ionic model is not a reasonable first description. Theoretically, these systems are attractive because, to a good approximation, it is valid to describe the resonance experiments, the optical spectra, and the static susceptibilities in terms of the orbital functions of a very small number of electrons acting in the environment of many more electrons.

Most of the researches into the superhyperfine structure (shfs) of transition-metal fluorides[12–18] have

[1] M. Tinkham, Proc. Roy. Soc. (London) **A236**, 535 (1956); **A236**, 549 (1956).
[2] W. Low, Phys. Rev. **109**, 256 (1958).
[3] B. Bleaney and W. Hayes, Proc. Phys. Soc. (London) **B70**, 626 (1957); W. Hayes and D. A. Jones, *ibid.* **71**, 503 (1958); W. Hayes, Disc. Faraday Soc. **26**, 58 (1958).
[4] C. G. Windsor, J. H. M. Thornley, J. H. E. Griffiths, and J. Owen, Proc. Phys. Soc. (London) **80**, 803 (1962); J. H. M. Thornley, C. G. Windsor, and J. Owen, Proc. Roy. Soc. (London) **A284**, 252 (1964).
[5] B. Bleaney and D. J. E. Ingram, Proc. Roy. Soc. (London) **A208**, 143 (1951).
[6] G. M. Zverev and A. M. Prokhorov, Zh. Eksperim. i Teor. Fiz. **39**, 57 (1960); **43**, 422 (1962) [English transls.: Soviet Phys.—JETP **12**, 41 (1961); **16**, 303 (1963)].
[7] E. Yamaka and R. G. Barnes, Phys. Rev. **125**, 1568 (1962).
[8] T. R. Sliker, Phys. Rev. **130**, 1749 (1963).
[9] A. Abragam and M. H. L. Pryce, Proc. Roy. Soc. (London) **A206**, 173 (1951); **A205**, 135 (1951).
[10] H. M. Gladney and J. D. Swalen, J. Chem. Phys. **42**, 1999 (1965).
[11] D. K. Rei, Fiz. Tverd. Tela **3**, 2223 (1961) [English transl.: Soviet Phys.—Solid State **3**, 1613 (1962)] shows in the case of Co^{++} in Al_2O_3 the difficulty of separating trigonal field and covalent binding factors.
[12] S. Ogawa, J. Phys. Soc. Japan **15**, 1475 (1960).
[13] R. G. Shulman and K. Knox, Phys. Rev. **119**, 94 (1960); Phys. Rev. Letters **4**, 603 (1960).
[14] A. Mukherji and T. P. Das. Phys. Rev. **111**, 1479 (1958).
[15] T. P. P. Hall, W. Hayes, R. W. H. Stevenson, and J. Wilkins, J. Chem. Phys. **38**, 1977 (1963); **39**, 35 (1963).
[16] R. G. Shulman and S. Sugano, Phys. Rev. **130**, 506 (1963); S. Sugano and R. G. Shulman, **130**, 512 (1963); K. Knox, R. G. Shulman, and S. Sugano, Phys. Rev. **130**, 520 (1963).
[17] M. Peter and J. B. Mock, Phys. Rev. **118**, 137 (1960).
[18] J. Ferguson, H. J. Guggenheim, H. Kamimura, and Y. Tanabe (to be published).

been concerned with closed or half-closed d-electron subshells in octahedral environments (d^3, d^5, and d^8 ions). As Thornley *et al.*[4] point out, Co^{++} differs from all these cases in that measures of both σ and π bonding are available. We anticipate that the noncubic environment of the substitution site in MgF_2 will provide comparative information about the inequivalent bonds. Although the spectra reported are of such complexity as to discourage their study, we found it possible to account for them in detail. The only previous analyses of spectra of comparable intricacy are the pioneering study by Tinkham[1] and more recent work on $ZnF_2:Mn^{++}$ by Clogston *et al.*[19]

Particular interest has been revived in the properties of $MgF_2:Co$ and CoF_2, through studies of the infrared and visible spectra in connection with the possibility of laser applications,[20] of antiferromagnetic resonance,[21] and of the NMR of Co^{59}.[22] The EPR information should prove complementary to these experiments.

Our analysis of the EPR is presented in several sections below. In Sec. II, the form and symmetry of the spin Hamiltonian is given from a description of the crystal symmetry and crystal-field theory. Following a brief description of the experimental methods and the over-all appearance of the spectra in Sec. III, the detailed analysis of the Zeeman effect and the cobalt-hyperfine interaction in Sec. IV serves as the background for the measurement and calculation of the F^{19} shfs in Sec. V. The calculations performed are direct diagonalizations of the spin Hamiltonian for a model problem. The relationship of the model to the full Hamiltonian and an explanation of the anomalies of the shfs by high-order perturbation theory are relegated to an Appendix. The spin-Hamiltonian parameters are reported in the concluding section, which also includes some very simple comments on the electronic structure of orthorhombic Co^{++} systems. Detailed theory is of necessity deferred to a later paper.

II. THE SPIN HAMILTONIAN

Magnesium fluoride is a crystal of the rutile structure (Fig. 1), with two metal ions per unit cell, each with only rhombic symmetry and equivalent to the other under a 90° rotation about the crystal c axis. Each cation is surrounded by a distorted octahedron of fluoride ions: two (axial) anions are displaced along a 110 crystal axis; four (equatorial) anions lie in the perpendicular plane in a rectangle with one side parallel to the c axis. The axial anions are slightly farther from

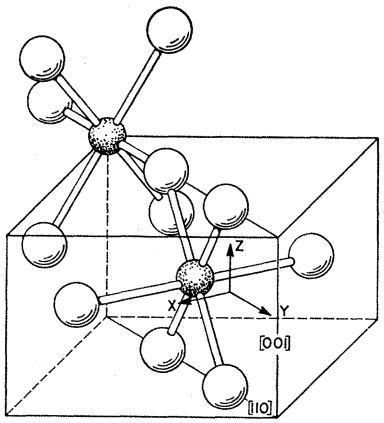

FIG. 1. Schematic of MgF_2, showing the two nonequivalent cation sites. The Cartesian axes used in this paper are identified. Dark balls represent cations, and white, anions.

the cation than the equatorial ions.[23] It is convenient to label directions relative to the cation sites as: z axis along the crystal c axis, x axis along the 110 line joining the two axial fluorides and y axis to complete the orthogonal triad. Cobaltous ions enter the lattice substitutionally for magnesium ions. The symmetry of the ions is such that any tensor quantity associated either with the cation or with the axial anions necessarily has its principal directions along the labeled axes. Tensors associated with the equatorial fluorides have one principal direction parallel to the x axis, but the others are not determined by symmetry.

In an octahedral field, the ground ^4F state of the cobaltous ion produces an orbitally degenerate $^4\Gamma_4$ ground manifold which is further split by the spin-orbit interaction to give a lowest Kramers doublet. This state is, of course, not further split in tetragonal or orthorhombic symmetry. Since the lowest excited state is more than 100 cm^{-1} above the ground state,[20,24] only transitions between components of the ground doublet can be seen in the electron-spin-resonance spectrum. But, the low excited states lie so close that the EPR may be observed only at very low temperatures. Since the only stable isotope of cobalt has nuclear spin $\frac{7}{2}$, the resonance spectrum may be described by an effective Hamiltonian

$$\mathcal{H}=\beta\mathbf{S}\times\mathbf{g}\times\mathbf{H}+\mathbf{S}\times\mathbf{A}^{Co}\times\mathbf{I}^{Co}, \qquad (1)$$

with effective spin $|S|=\frac{1}{2}$ and nuclear spin $|I^{Co}|=\frac{7}{2}$. Here, nuclear Zeeman interactions are omitted because transitions changing the nuclear spin have very low intensity and because the shifts in the allowed ($\Delta I_z=0$), lines induced by these terms are negligible. Also, nuclear-quadrupole interactions are negligible,[9] and, therefore, are omitted. Each of the eight lines expected from Eq. (1) is further split by the hyperfine interactions of the electron spin with the magnetic moments of the

[19] A. M. Clogston, J. P. Gordon, V. Jaccarino, M. Peter, and L. R. Walker, Phys. Rev. **117**, 1222 (1960).
[20] L. F. Johnson, R. E. Dietz, and H. J. Guggenheim, Appl. Phys. Letters **5**, 21 (1964).
[21] H. Kamimura and Y. Tanabe, J. Appl. Phys. **34**, 1239 (1963); H. Kamimura, *ibid.* **35**, 844 (1964); P. L. Richards, *ibid.* **34**, 1237 (1963); M. E. Lines, Phys. Rev. **137**, A982 (1965).
[22] V. Jaccarino, Phys. Rev. Letters **2**, 163 (1959).
[23] The lattice parameters of all the fluorides isomorphous to rutile are given by W. H. Bauer, Acta Cryst. **9**, 515 (1956); **11**, 488 (1958).
[24] R. Newman and R. M. Chrenko, Phys. Rev. **115**, 1147 (1959).

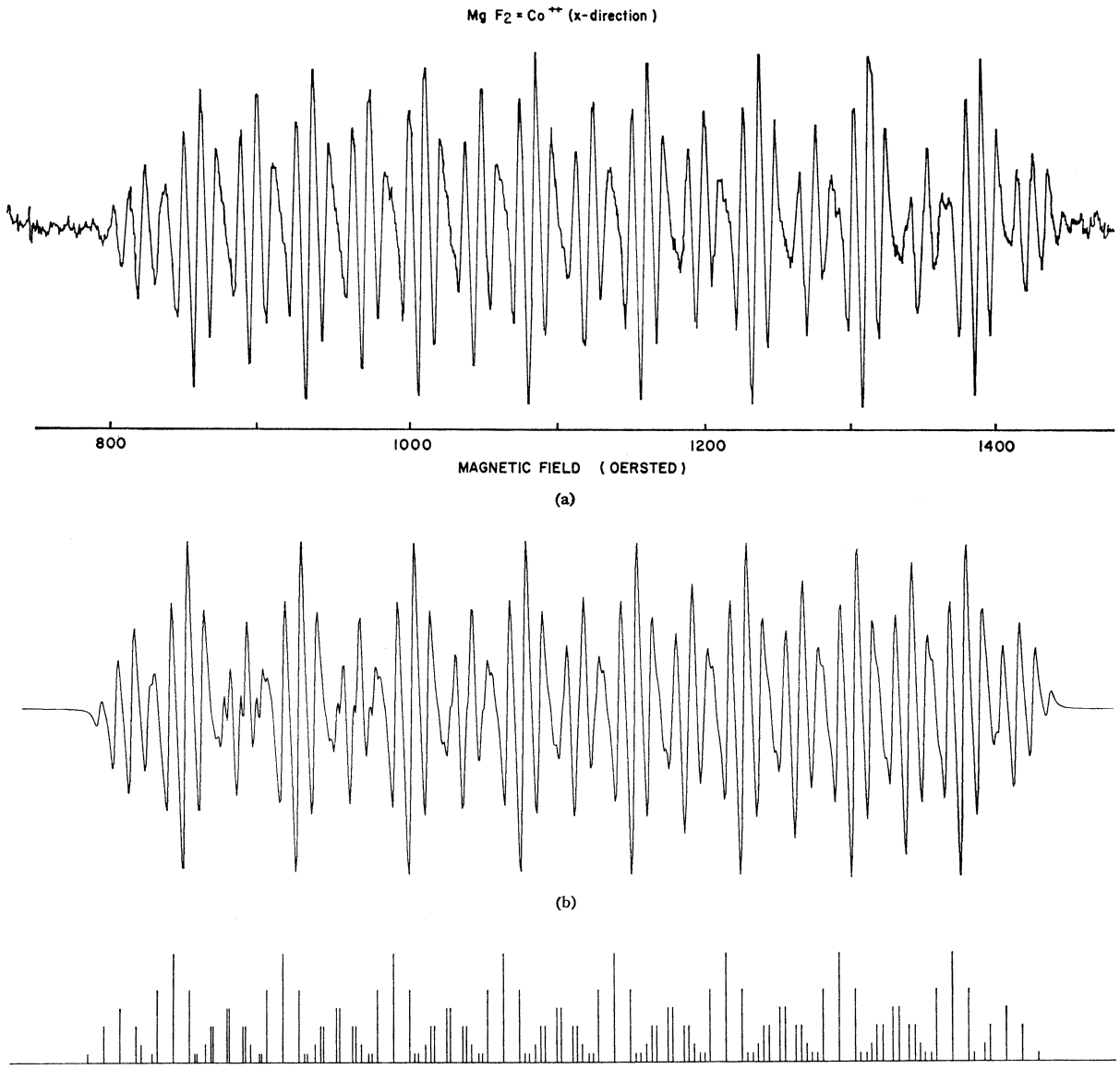

FIG. 2. (a) Experimental X-band EPR spectrum of Co^{++}:MgF_2 with $H\|[110]$. This is the low-field spectrum associated with the x axis. (b) Computed spectrum corresponding to (a). The "stick diagram" in the lower portion indicates the line positions and intensities.

neighboring fluorine nuclei (spin $\frac{1}{2}$). For the ith neighboring fluorine nucleus, an additional term

$$\mathcal{H}_{\text{hfs}}{}^{i}=\mathbf{S}\times\mathbf{A}^{i}\times\mathbf{I}^{i} \tag{2}$$

must be added to the Hamiltonian Eq. (1). The interaction of any particular F^{19} nucleus is equal to that of the nucleus at the inversion point about the cation.[25] Not even the relative signs of the hyperfine parameters can be derived from our resonance experiments. This has been shown in perturbation formulas,[26] but is also an easily demonstrated, exact theorem for the Hamiltonian (1).[27]

Because MgF_2 has two substitution sites, the principal tensor directions, x and y (Fig. 1), may be assigned only by detailed analysis of the equatorial fluorine hyperfine interactions. If the external magnetic field is in the yz plane, these are not in general equivalent, so that the spectra are expected to have splittings not otherwise explicable. Also, each F^{19} hyperfine tensor

[25] Below the hyperfine tensor for the equatorial fluorides is denoted $\mathbf{A}^{4F}$; that for the axial, $\mathbf{A}^{2F}$.

[26] W. Low, *Paramagnetic Resonance in Solids* (Academic Press Inc., New York, 1960), p. 60.

[27] H. C. Heller, J. Chem. Phys. 42, 2611 (1965), shows that relative signs for different magnetic nuclei may be found by zero-field resonance.

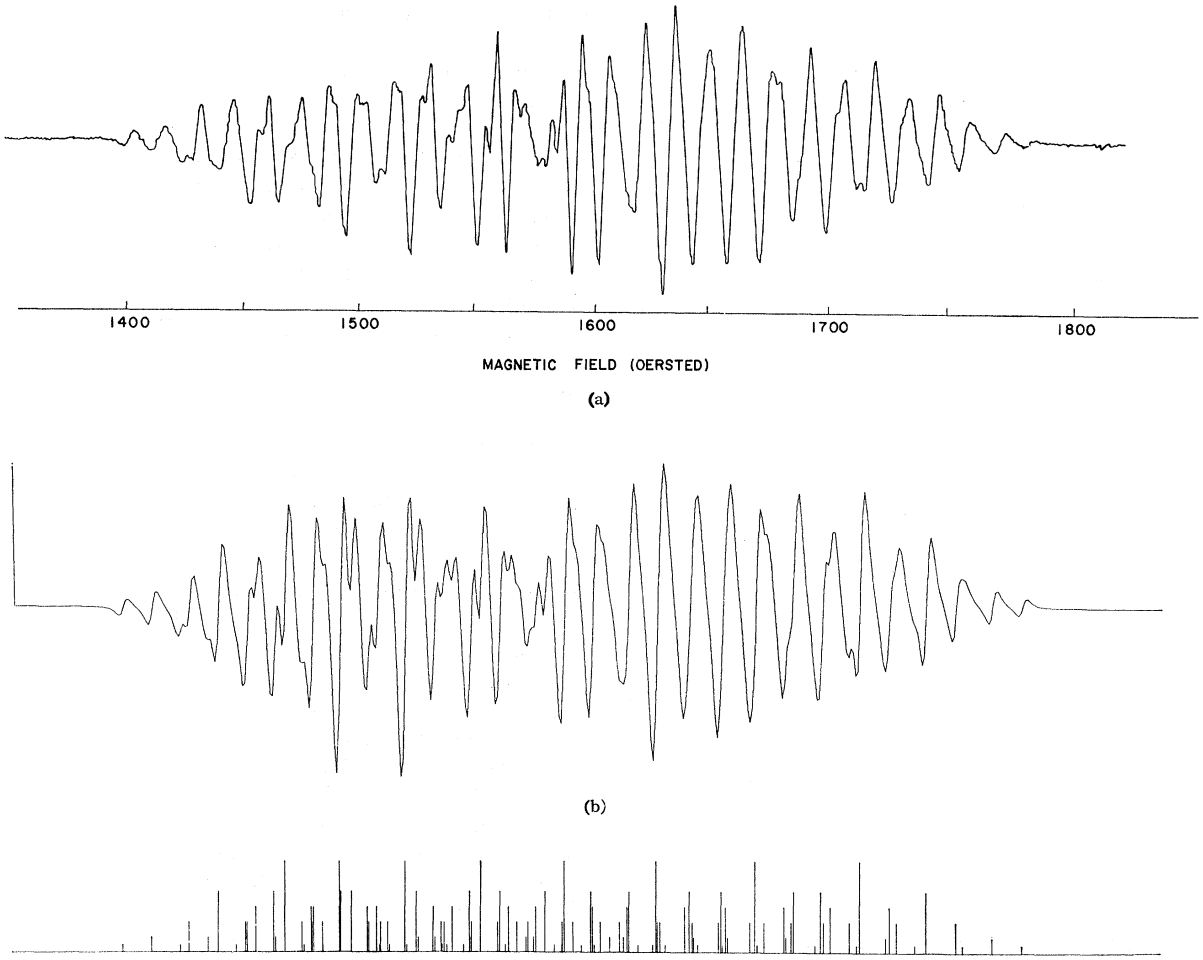

FIG. 3. (a) Experimental X-band EPR spectrum of $Co^{++}:MgF_2$ with $H\|[001]$ (the z spectrum). (b) Computed spectrum corresponding to (a).

should be approximately an ellipsoid of revolution about the bond direction.[28]

III. EXPERIMENTAL METHOD

Our sample was a single, uncolored crystal of optical quality MgF_2, nominally doped to 0.1%.[29] As well as the EPR spectrum of cobalt, which is easily recognized by its temperature dependence, large g-tensor anisotropy and characteristic eightfold hyperfine structure, the sample showed a weak spectrum of Mn^{++}, which did not interfere with the analysis. The spectra were observed with a conventional X-band superheterodyne spectrometer with 400-cycle/sec phase-sensitive detection.[30] Sample orientation was achieved very conveniently and precisely ($\pm 0.2°$) by mounting the crystal on a rotating platform on the narrow side of a TE_{011} rectangular cavity—the rotation axis of the crystal was then perpendicular to that of the rotating 12-in. electromagnet. The platform was driven by a protractor outside the liquid-helium Dewars.

IV. ANALYSIS OF THE SPECTROSCOPIC SPLITTING AND COBALT hfs

The regularity of the x spectrum (Fig. 2) in spacing and intensity is remarkably reminiscent of the spectra of organic free radicals in liquid solution, which is unusual because the hyperfine interactions are not small, but induce a 600-G wide spectrum centered at about 1100 G. The regularity occurs because the largest contributions of the cobalt hyperfine tensor lie on the diagonal (in a strong-field representation). The off-diagonal interactions, linear in A_y^{Co} and A_z^{Co}, barely affect the uniformity of the spacing of the $(M_{Co},0,0)$

[28] For example, for $Mn^{++}:ZnF_2$, (Ref. 19), the component along the bond of the axial fluorines exceeds the perpendicular components by 70%. The perpendicular values differ by only about 4%.

[29] The crystal was obtained from Optovac, Inc.

[30] J. P. Goldsborough and T. R. Koehler, Phys. Rev. 133, A135 (1964).

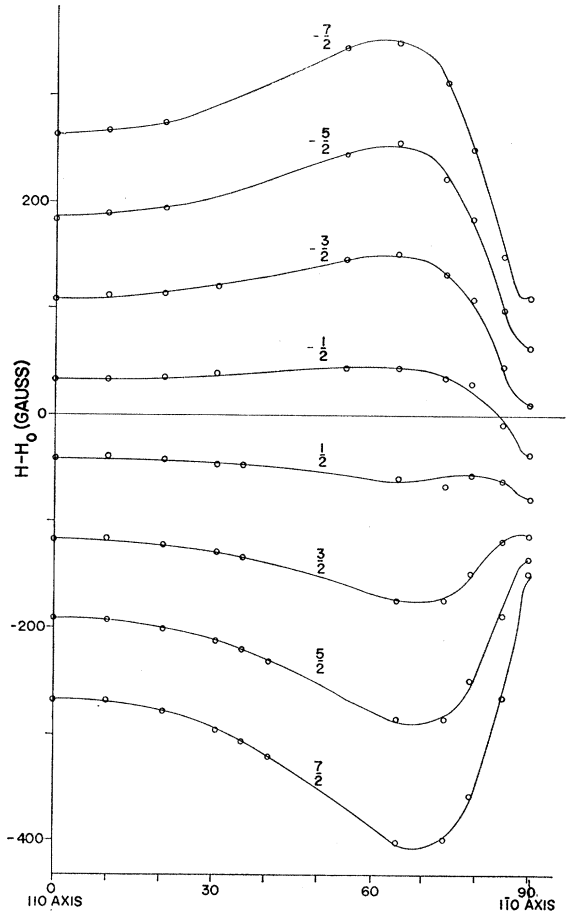

FIG. 4. Angular variation of the cobalt hfs magnetic field in the xy plane. The curves are calculated from the principal direction measurements listed in Table I. The circles represent measured line positions. To eliminate the large shift of each pattern because of the large anisotropy of the g tensor, we have plotted the difference of the resonance field and $H=h\nu/g\beta$, where $g^2=g_x^2\sin^2\theta\cos^2\phi+g_y^2\sin^2\theta\sin^2\phi+g_z^2\cos^2\theta$. To eliminate the effects of angle errors (to which the Zeeman effect is much more sensitive than the hyperfine splitting), we have fitted the $(\frac{1}{2},0,0)$ lines to the theoretical curves. Cobalt spin labels designate the lines.

lines.[31] This spacing ranges from 74.2 G between $(+\frac{7}{2},0,0)$ and $(+\frac{5}{2},0,0)$ to 76.8 between $(-\frac{5}{2},0,0)$ and $(-\frac{7}{2},0,0)$. Because $\frac{1}{2}A_x^{\mathrm{Co}}\approx A_x^{2\mathrm{F}}>3A_x^{4\mathrm{F}}$, any overlap of lines occurs in a regularly constructive fashion, so that the assignment of the spectrum is obvious. The peak-to-peak line intensities are within 10% of the statistical weights expected.

Unfortunately, the spectra are not always so simple. Since the cobalt hyperfine splitting is not uniform for most directions of the static magnetic field, and since the fluorine hyperfine interactions are of the same order of magnitude as the cobalt splitting, many of the spectra are irregular and difficult to assign. For instance, in the z spectrum (Fig. 3) the cobalt hyperfine spacing varies from 24 G at the low-field end of the spectrum to 46 G at the high-field end. This is complicated by the fact that the hyperfine interaction $A_z^{4\mathrm{F}}$ has the same order of magnitude as A_z^{Co}.

Three machine programs, briefly described in Appendix A, have been invaluable in the assignment of the spectra and the precise determination of the Hamiltonian parameters. EPR diagonalizes Eq. (1) to predict the resonance fields; PARA adjusts the parameters of the spin Hamiltonian to fit observed resonances, and HYP calculates and plots on digital-to-analog equipment spectra of Lorentzian lines calculated from estimates of the positions of the $(M_{\mathrm{Co}},0,0)$ lines and the fluoride hyperfine spacings.[32,33] EPR and PARA were not only convenient, but essential to the analysis reported. For arbitrary field directions, perturbation formulas for Eq. (1) are not available, and, if developed, would be tedious to apply and not sufficiently accurate.

Partly to make possible and to verify the assignment of the $(M_{\mathrm{Co}},0,0)$ lines, and partly to investigate anomalies in the fluoride hyperfine interaction, we studied the angular variations in the 110 and 001 planes. The measured positions agree with the calculated ones within the small errors expected to be generated by overlapping lines. The largest variations with angle occur in the xy plane (Fig. 4), where the spectrum ranges from 660 G wide along (90°,0°) to 950 G along (90°,74°) to 420 G along (90°,90°).[34] At least to terms of second order, the width of the spectrum is determined by the first-order hyperfine interaction. The observed behavior then is easily accounted for by the angular dependence of the first-order term. The details of the spacing for an axial Hamiltonian have been discussed by Bleaney and Ingram.[5] They are, however, somewhat ambiguous in their description.

[31] Because nuclear spins are conserved in the EPR transitions, we can unambiguously designate lines with the labels $(M_{\mathrm{Co}}, M_a, M_e)$, in terms of components along the effective field direction of the cobalt nuclear spin, of the effective total spin of the axial fluorines, and of the effective total spin of the equatorial fluorines. The labels are valid even when first-order perturbation theory is not.

[32] It has been our experience that it is essential to verify the assignments and the spin-Hamiltonian parameters by comparison of calculated with observed spectra. Errors in the estimates of fluorine hyperfine spacings of only a quarter of the line halfwidth significantly distort the calculated spectra. On more than one occasion an incorrect assignment with a "stick diagram" has been exposed by unsuccessful attempts to reproduce the spectrum in calculation. When there are many overlaps of lines and groups of lines, small discrepancies between a "stick diagram" and the observed spectrum are hard to detect but may indicate qualitative errors which accompany a complete misinterpretation. In particular, observed line intensities may be quite different from statistical weights when many lines interfere either constructively or destructively. It is usually possible to plot a calculated spectrum which reproduces each bump and shoulder of the observed spectrum. Small errors in line positions or width occasionally separate shoulders of lines a bit too much; such discrepancies do not indicate major errors, but any larger disagreements, such as a single missing or extra line, almost certainly indicate a misassignment even though the over-all appearance may be satisfactory.

[33] J. D. Swalen and H. M. Gladney, IBM J. Res. Develop. 8, 515 (1964), list many programs for EPR data reduction.

[34] We designate the magnetic field orientation for some spectra using the polar angles (θ,ϕ). The principal axes are, respectively: $x(90°,0°)$; $y(90°,90°)$; and $z(0°,0°)$.

Although with the field along the principal directions, the large separations occur always towards high fields, it is possible that in intermediate directions the second-order perturbation term proportional to $\sin^2\theta\cos^2\theta$ causes the largest splittings to appear at the low-field end of the spectrum.

Near the (90°,90°) orientation the spacings at the high-field end of the spectrum are insensitive to small changes of orientation. But at the low-field end, the spacing between $(\frac{7}{2},0,0)$ and $(\frac{5}{2},0,0)$ varies from 13.2 to 34.6 to 47.5 G at (90°,90°), (90°,89°), and (90°,88°), respectively. For this reason, the values g_y and A_y^{Co} quoted below were derived by fitting the five groups of lines of the high-field end of the y spectrum only. The data for the xz and yz planes are quite similar to those in the xy plane except that the variations are much smaller.

One or two conclusions based on the analysis of the Co hyperfine spectrum are relevant to the following discussion of the fluorine shfs. Although the off-diagonal elements of $\mathbf{S}\times\mathbf{A}^{Co}\times\mathbf{I}^{Co}$ produce large shifts of lines from their first-order positions, in some respects the wave functions are surprisingly similar to the first-order functions. For instance, transitions with simultaneous cobalt nuclear spin flips, forbidden in first-order perturbation theory, still have less than 10^{-3} of the intensity of the allowed transitions. Therefore, the complexity of the spectra presented is to be explained in terms of fluorine hyperfine interactions. Also, the electron spin along the usual quantization direction[35] is almost a good quantum number; the mixing of the $m_s=-\frac{1}{2}$ state into the $m_s=\frac{1}{2}$ state is always less than 1%, so that to convert fluorine hyperfine spacings ΔH, observed in oersteds, to energy units the simple formula $A_{\text{eff}}=\beta g_{\text{eff}}\Delta H$ is adequate.

V. FLUORINE HYPERFINE STRUCTURE

For a general direction of the external magnetic field (and hence a general direction of the electron-spin quantization) each of the eight lines from the Hamiltonian Eq. (1a) can be split by the nearest-neighbor superhyperfine interactions [Eq. (1b)] into 27 components with intensities determined simply by the statistical weights of the nuclear-spin states. If, on the other hand, the magnetic field lies either in the xy plane, or in the xz plane, the quantization of the electron spin lies in the same plane, and the hyperfine interactions of the four equatorial fluorides become equal so that each of the eight lines split at most into 15 components.

Figure 2 illustrates particularly clearly the shfs. Each $(M_{Co},0,0)$ line is split by the pair of axial fluorides into three evenly spaced patterns with intensities 1:2:1, and each of these groups is split by the four equatorial fluorides into five evenly spaced lines with intensities 1:4:6:4:1. The spectra with the magnetic field in the xz plane or the xy plane may all be assigned with this structure, and become complicated mainly because different groups of lines overlap. The fluorine hyperfine parameters, with the exception of the off-diagonal part of $\mathbf{A}^{4F}$, may be measured from the principal-axis spectra. In the yz plane, we observe additional splitting because the equatorial fluorides are no longer all equivalent. This observation unambiguously identifies the smallest principal value of the g tensor with the y axis, and the largest with the x axis. The measured angular variation of the hyperfine interactions of the two pairs of equatorial fluorines is fit with a first-order calculation[36] in Fig. 5, which indicates one more potential ambiguity. The experiment does not show whether the minimum or the maximum principal value of $\mathbf{A}^{4F}$ is to be associated with the bond direction. The analogy with the axial fluorides seems to indicate that the tensor approximates a prolate ellipsoid of revolution about the bond direction.

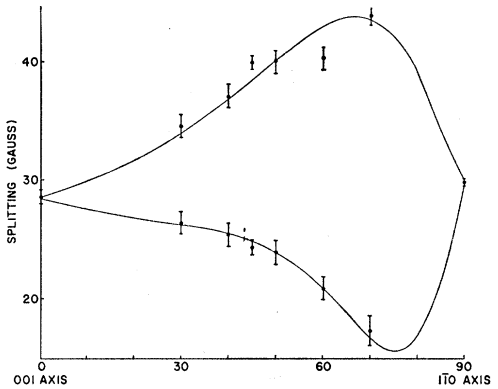

FIG. 5. Shfs of the equatorial fluorines for magnetic fields in the yz plane. The experimental data are taken from the $M_{Co}=-\frac{7}{2}$ group of lines. That they are not very complete or particularly precise reflects the problem of overlapping lines. The curve is drawn from a first-order perturbation calculation with $A_z^{4F}=0.1617$, $A_y^{4F}=0.0756$, $A_{yz}^{4F}=0.0491$ kMc/sec. The lower portion occurs for the colatitude θ positive and the upper portion for θ negative. Since the effective colatitude for one pair of equatorial fluorines is the negative of that for the other pair, both splittings occur in each spectrum so that the curve is folded into one 90° range.

The fluorine hyperfine interactions are small compared with the spectroscopic splitting, so that one

[35] See, W. Low, Ref. 26, p. 56.

[36] Where the angle between the principal z axis of the hyperfine tensor and the crystal c axis is ξ, it is easily shown that the principal components are related to the components in the crystal-axis system by

$$A_{zP}^{4F}=A_z\cos^2\xi+2A_{yz}\cos\xi\sin\xi+A_y\sin^2\xi$$

and

$$A_{yP}^{4F}=A_z\sin^2\xi-2A_{yz}\cos\xi\sin\xi+A_y\cos^2\xi,$$

with

$$\xi=\tfrac{1}{2}\arctan[2A_{yz}/(A_z-A_y)].$$

If the magnetic field is oriented along $(\theta,90°)$ the first-order hyperfine interaction K is given by

$$K^2=(A_{zP}^{4F})^2\cos^2\sigma'+(A_{yP}^{4F})^2\sin^2\sigma',$$

with

$$\sigma'=\sigma+\xi \quad \sigma=\tan^{-1}[(\tan\theta)g_y/g_z].$$

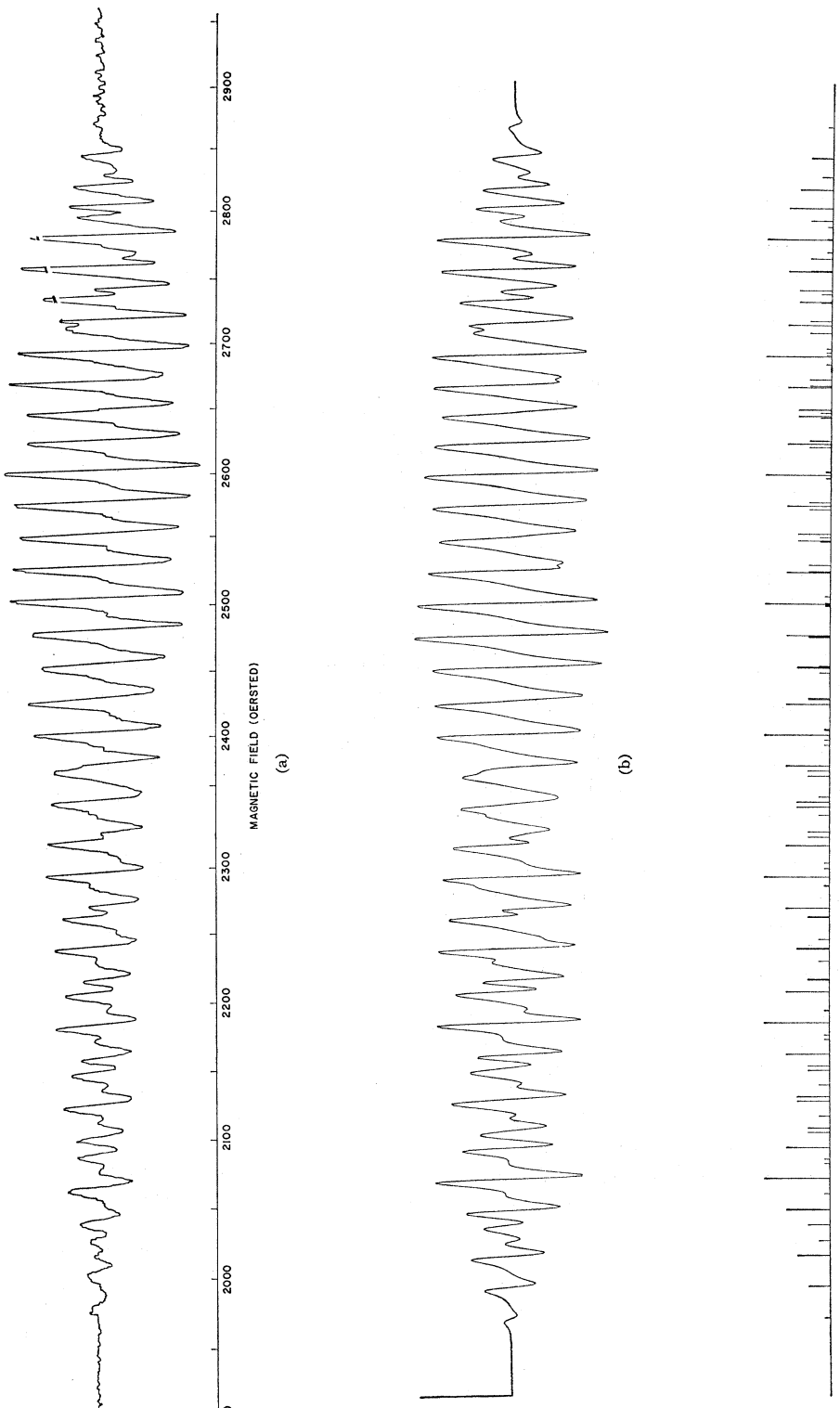

FIG. 6. (a) Experimental spectrum of Co^{++}:MgF_2 with H along (90°,74°). (b) Computed spectrum at (90°,74°).

would expect that first-order perturbations would adequately predict the angular variation of the splitting. In particular, first-order theory requires that the fluorine hyperfine spacing should be independent of the cobalt spin label of the transition. However, many of the spectra, including the y spectrum, could not be assigned on this assumption.[37] The anomaly is illustrated particularly clearly by the spectrum at (90°,74°) (Fig. 6). The group of lines on the low-field side of the $(\frac{7}{2},0,0)$ line should be a mirror image of the group on the high-field side of the $(-\frac{7}{2},0,0)$ line. (In these regions, lines belonging to other cobalt spin numbers do not occur.) The end groups can be fit only if one assumes that the spacing between $(+\frac{7}{2},+1,0)$ and $(+\frac{7}{2},0,0)$ is about 59 G, and that between $(-\frac{7}{2},0,0)$ and $(-\frac{7}{2},-1,0)$ is about 38 G; these values bracket the separation predicted by first-order perturbation theory.

Complete diagonalization of the entire spin Hamiltonian, including fluorine hyperfine interactions is an unreasonably expensive calculation. To model the anomalies of the fluorine hyperfine spacings, consider the EPR spectrum of a hypothetical CoF fragment. The appropriate spin Hamiltonian is

$$\mathcal{H}^M=\beta\mathbf{S}\times\mathbf{g}\times\mathbf{H}+\mathbf{S}\times\mathbf{A}^{Co}\times\mathbf{I}^{Co}+\mathbf{S}\times\mathbf{A}^{F}\times\mathbf{I}^{F},$$

with

$$|I^{Co}|=\tfrac{7}{2}\quad|I^{F}|=\tfrac{1}{2}. \tag{3}$$

The tensor $\mathbf{A}^F$ is to be set equal either to $\mathbf{A}^{2F}$ or to $\mathbf{A}^{4F}$, according to whether one wishes to calculate the splitting of the axial or of the equatorial fluorines. Each calculation involves a 32×32 diagonalization. In Appendix B, we show that, to a good approximation, calculations for shfs splittings in CoF may be directly applied to $(CoF^6)^{4-}$. At the same time the anomalous variations of the splitting are traced principally to fourth-order perturbations, which become important because of near degeneracies in certain sets of zero-order levels. In Fig. 7 we compare fluorine hyperfine separations calculated for CoF with measured line separations. In the calculated spectra [Figs. 2(b), 3(b), and 6(b)] this variation has been included; it has negligible effects in the x spectrum, very small but noticeable effects in the z spectrum and very large effects in the (90°,74°) spectrum. All these figures show extremely good agreement between the calculated and observed spectra.

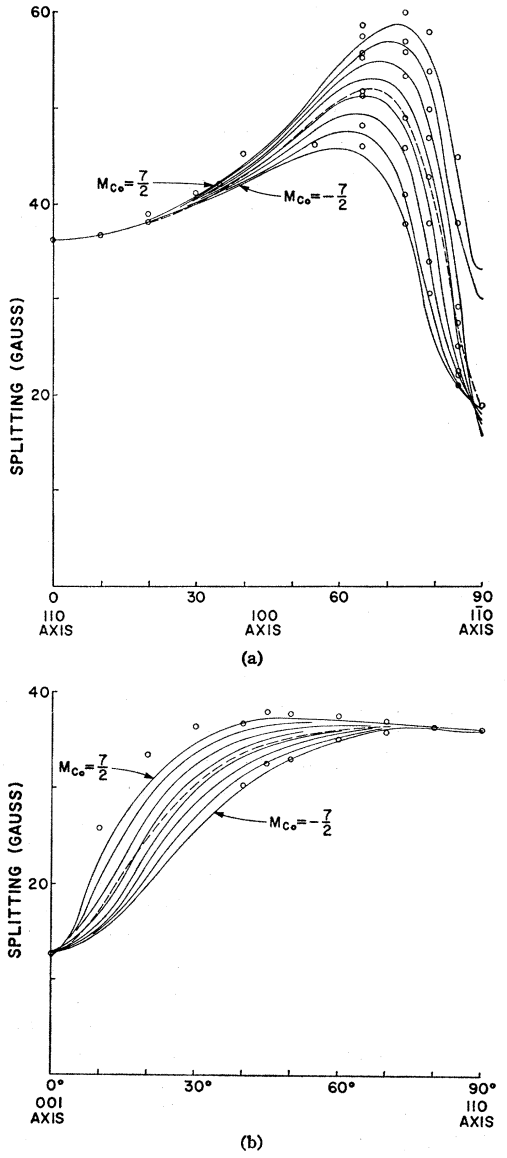

FIG. 7. Variation of the axial fluorine hyperfine splittings with magnetic field orientation and cobalt spin number. The curves are calculated from the principal values by the algorithm described in the text. Measurement of the splittings in the central regions of the spectra is tedious and unreliable, so that with the exception of one series, only the values for cobalt spin number $\pm\frac{7}{2}$ have been measured. The effect for the equatorial fluorines is similar but smaller. ---- calculated by first-order perturbation theory. (a) In the xy plane. At each angle, the order of the experimental splittings corresponds to the order of the theoretical curves. (b) In the xz plane.

VI. RESULTS AND DISCUSSION

The final values of the spin-Hamiltonian parameters appear in Table I. Compared with the parameters available for $ZnF_2:Co$,[1] the values for $MgF_2:Co$ are just outside the range of insignificant differences. That Tinkham's estimates of the values of A_y^{Co} and A_z^{Co}, which he did not observe, are so close to our observation suggest that the most important features of a careful theory are included in his very simple treatment of the relationship of the g and A tensors. His estimate of g_y, based on the approximate constancy of $(g_x+g_y+g_z)$ for Co^{++} in a large range of crystalline environments is significantly different from our measured value. The two shfs parameters reported for ZnF_2 are nearly the

[37] The anomaly is distinct from the effect reported by Clogston *et al.* (Ref. 19), who report a case when F^{19} nuclear spin quantization is not preserved.

TABLE I. Spin-Hamiltonian parameters.

	MgF_2:Co^{++}[a]	ZnF_2:Co^{++}[c,d]	TiO_2:Co^{++}[f]	NaF:Co^{++}[g]
g_x	6.0327±0.0007	6.05±0.01	5.88±0.02	5.7
g_y	2.2970±0.0004	(2.6)	2.19±0.005	3.3
g_z	4.2391±0.0005	4.1 ±0.1	3.75±0.01	4.3
A_x^{Co}	637.1 ±0.4 Mc/sec	651.0 ±6.0 Mc/sec	450.0 ±6.0 Mc/sec	750.0 Mc/sec
A_y^{Co}	123.3 ±0.8	(129.0)	120.0 ±6.0	250.0
A_z^{Co}	210.0 ±0.4	(201.0)	78.0 ±3.0	...
A_x^{2F}	308.0 ±5.0	...		
A_y^{2F}	59.4 ±0.9	...		
A_z^{2F}	75.8 ±2.0	...		
A_x^{4F}	92.0 ±3.0	96.0 ±3.0[e]		
A_y^{4F}	76.0 ±6.0[b]	...		
A_z^{4F}	162.0 ±4.0[b]	163.0 ±6.0[e]		
A_{yz}^{4F}	49.0 ±6.0[b]	...		

[a] This paper. The precisions of g and A^{Co} are determined by the internal errors of fitting eight lines in each principal direction. Those of A^{2F} and A^{4F} are limited by errors of spacings introduced by overlapping lines.
[b] The expectations of this splitting when the field is along the z and y axes are more precise than these values. They are 169±3 and 90.2±1 Mc/sec, respectively.
[c] M. Tinkham, Ref. 1. The bracketed values were estimated with a simple theory. Our assignment of the directions differs from Tinkham's.
[d] Kamimura (Ref. 2) quotes unpublished measurements by D. Shaltiel for ZnF_2:Co^{++} with $g_z=6.09$, $g_y=2.33$, $g_z=4.25$. Hyperfine data are not available. More recently, Lines (Ref. 21) quotes unpublished measurements by J. C. Hensel which have $A_z^{Co}=217$ Mc/sec.
[e] Tinkham does not assign these spacings to one or the other class of fluorides. His A_z^{4F} is the first-order splitting on the z axis, and includes a contribution from A_{yz}^{4F}.
[f] References 6 and 7.
[g] Reference 3.

same as those for MgF_2. It would be interesting to repeat our measurements with ZnF_2 as host to complete the comparison. If, as we suspect, the details of the geometry in the neighborhood of Co^{++} are dominated, not by the host lattice parameters, but by the bonding propensities of the impurity ion, the spin-Hamiltonian parameters should be almost identical for the two hosts.[38] We have made preliminary measurements of the EPR of Mn^{++} in MgF_2 which indicate that while the shfs is very similar to that reported in ZnF_2,[19] the fine structure constants differ by as much as 25%.

Observation of the off-diagonal part of A_x^{4F} confirms our assignment from less conclusive evidence of spin-Hamiltonian directions to bond directions of the crystal. The principal values of the equatorial F^{19} hyperfine tensor are (92, 53, 184) Mc/sec. By analogy with the axial F^{19} tensor, the large component may be assigned to the direction closest to the bond. However, to our surprise, the maximal principal axis is not along the bond, but is tilted 24.4±1° from the c axis; the bond direction makes an angle of 40.2° with the c axis in MgF_2 (in CoF_2 it is 39°). In contrast, for ZnF_2:Mn^{++}, the principal axis lies 38° from the c axis[19]—which is indistinguishable from the bond direction. Presumably the altered direction for Co^{++} is related to the large g-tensor anisotropy.

The reported spectra are quite similar to previous ones in rhombohedral environments, and are suggestive of solutions to some unresolved problems in the literature. In Table I we have included for comparison two of the most similar spectra. For TiO_2:Co^{++} the ambiguity of the directions is not resolved by experimental data. Our assignment, based on the analysis of A^{4F} and the analogy of similar Zeeman and Co-hyperfine tensors, confirms the opinion of Zverev and Prokhorov,[6] but is at odds with that of Yamaka and Barnes,[7] who base their decision on inconclusive arguments from crystal-field theory. The partially analyzed spectrum of the low-symmetry site of NaF:Co^{++}[3] is closely related to that of Co^{++} in the MgF_2 substitution site. With EPR and PARA, the analysis could readily be completed to describe the well-resolved F^{19} shfs.

The theory of the shfs required for $(CoF_6)^{=}$ involves a number of complications over any similar case previously treated and will, therefore, be deferred to another paper. For the present we content ourselves with relatively simple comments within the crude theories offered by Abragam and Pryce[9] and by Tinkham.[1] These comments are occasioned by our completion of the set of spin-Hamiltonian parameters, our reassignment of the principal axes relative to the site geometry, and the suggestions these data engender about the interpretation of the resonance experiments for the other rhombohedral Co^{++} systems. If a small contribution from the ^4P atomic state is neglected, and if the tetragonal and rhombic parts of the crystal field are treated in first-order perturbation theory, the spectroscopic splitting factor may be decomposed into spin and orbital parts[1]

$$\begin{aligned} g_x &= g_{Sx}+kg_{Lx}{}^0=(10-8a)/3+k(1-2a), \\ g_y &= g_{Sy}+kg_{Ly}{}^0=(10+4a+4r)/3+k(1+a+r), \\ g_z &= g_{Sz}+kg_{Lz}{}^0=(10+4a-4r)/3+k(1+a-r). \end{aligned} \quad (4)$$

Here, a and r arise from the axial and rhombic parts

[38] The shfs parameters are especially sensitive to the bond distance, since they are roughly proportional to $(S+\gamma)^2$, and since the orbital overlap integrals and the covalent mixing parameter γ should vary roughly exponentially in the bond length (Ref. 19).

of the field; the orbital reduction factor[39] ($k \leq 1$) should show spin-density transfer from the paramagnetic ion to the ligands. In Table I we have fit a, r, and k to the g tensor; calculations of the hyperfine tensor are made with[1,40]

$$A_i = N^2 P[(g_L{}^0)_i - \tfrac{1}{2}\kappa(g_S)_i], \quad i = x, y, z \tag{5}$$

where we arbitrarily choose[9] $P(\equiv \gamma\beta\beta_N\langle r^{-3}\rangle) = 0.0225$ $cm^{-1} = 675$ Mc/sec and $\kappa = 0.325$. We could treat κ as an adjustable parameter, but this hardly seems justified by the scanty data. For $MgF_2:Co^{++}$ the values of $\mathbf{A}^{Co}$ correspond fairly well to the experimental values (Table I). The orbital reduction $k = 0.86$ is somewhat less than the value assumed by Tinkham and the $N^2 < k$ relation seems to hold. The agreement is poorer for the other host materials; in some cases the parameters are quite unreasonable. We cite these data to show the necessity of a careful re-examination of the theory.

ACKNOWLEDGMENTS

Many members of the Physics Department of the IBM San Jose Research Laboratory contributed to this research by patient listening and discussion. More direct contributions were made by Dr. K. E. Rieckhoff, who read and criticized the final manuscript, and by Tad Kuga, who performed most of the experiments. I am particularly grateful to Dr. J. D. Swalen for many suggestions and long discussions over a period of many months, and for invaluable comments on the manuscript.

APPENDIX A: MACHINE COMPUTATIONS IN THE SPECTRAL ANALYSIS

EPR uses the iterative Newton-Raphson method to find, for a specified g tensor and cobalt hyperfine tensor [Eq. (1a)], the resonance magnetic fields H by solving

$$W_i(H,\theta,\phi) - W_j(H,\theta,\phi) = h\nu. \tag{6}$$

Here W_i is the ith eigenvalue of (1) for the magnetic field orientation specified by the colatitude θ and the azimuth ϕ.[34] The resonance field calculations include calculations of the derivative of the resonance field with respect to the microwave frequency. The latter datum is useful for small corrections of observed fields to some standard microwave frequency and for conversion of hyperfine spacings in field units to those in frequency units.

Given a table of observed resonance fields at specified angles, PARA[41] refines an estimate of the spin-Hamiltonian parameters to give a least-squares fit of the observations. The method used is to invert the linear relationship of first-order deviations of the parameters to first-order deviations of resonance frequencies. Estimates of parameter errors arising from internal inconsistencies of the observations are included in the output.

EPR and PARA have more general capabilities than are implied by their application to the Hamiltonian, Eq. (1). In their present version they may be applied to any member of the class of spin Hamiltonians

$$\begin{aligned}\mathcal{H} = {} & \beta \mathbf{S}\times\mathbf{g}\times\mathbf{H} + D[S_z^2 - \tfrac{1}{3}S(S+1)] + E(S_x^2 - S_y^2) \\ & + \frac{a}{6}[S_x^4 + S_y^4 + S_z^4 - \tfrac{1}{3}S(S+1)(3S^2+3S-1)] \\ & + b[35S_z^4 - 30S(S+1)S_z^2 + 25S_z^2 \\ & \qquad - 6S(S+1) + 3S^2(S+1)^2],\end{aligned} \tag{7}$$

for any symmetry and any effective spin up to $S = \frac{5}{2}$. Moreover, the programs are constructed to facilitate extension to other forms of spin Hamiltonians by the addition of appropriate algorithms.

APPENDIX B: CALCULATION OF THE ANOMALOUS SHFS

In this Appendix, we first of all examine the Hamiltonian appropriate to CoF [Eq. (3)] in perturbation theory to describe the interactions responsible for the anomalous shfs, and then employ the perturbation theory to show how calculations for CoF may be employed in analyzing the spectra of CoF_6.

Examine, for example, the eigenstates of $\mathcal{H}^M$ when the magnetic field is along the principal axis of the minimal component of the g tensor, in the case when $\mathbf{A}^F \equiv \mathbf{A}^{2F}$, for $H = 2.955$ kG. Where $|m_s m_{Co} m_F\rangle$ is a strong-field basis function appropriate to $\mathcal{H}^M$, the eigenstate which has the largest mixing of basis states has the wave function

$$\begin{aligned}|M_s = \tfrac{1}{2}, M_{Co} = \tfrac{5}{2}, M_F = \tfrac{1}{2}\rangle \\ = 0.7796|\tfrac{1}{2}\,\tfrac{5}{2}\,\tfrac{1}{2}\rangle + 0.0562|-\tfrac{1}{2}\,\tfrac{3}{2}\,\tfrac{1}{2}\rangle + 0.0484|-\tfrac{1}{2}\,\tfrac{7}{2}\,\tfrac{1}{2}\rangle \\ + 0.2920|\tfrac{1}{2}\,\tfrac{1}{2}\,\tfrac{1}{2}\rangle + 0.0376|-\tfrac{1}{2}\,\tfrac{5}{2}\,-\tfrac{1}{2}\rangle \\ + 0.4725|\tfrac{1}{2}\,\tfrac{7}{2}\,-\tfrac{1}{2}\rangle + 0.2619|\tfrac{1}{2}\,\tfrac{3}{2}\,-\tfrac{1}{2}\rangle \\ + 0.0501|\tfrac{1}{2}\,-\tfrac{3}{2}\,\tfrac{1}{2}\rangle + 0.0691|\tfrac{1}{2}\,-\tfrac{1}{2}\,-\tfrac{1}{2}\rangle + \cdots.\end{aligned} \tag{8}$$

Consider the off-diagonal parts of $\mathcal{H}^M$ as a perturbation on the diagonal portions. Then the origin of the important contributions to the wave function may be indicated diagrammatically.[42] The first-order cobalt-spin corrections, Fig. 8(a), are smaller than the second-order cobalt-spin correction, Fig. 8(b), because the latter contribution includes a small energy denominator. For the same reason the first-order fluorine spin correction,

[39] K. W. H. Stevens, Proc. Roy. Soc. (London) **A219**, 542 (1953).

[40] κ measures the admixture of unpaired s electrons on the central ion. N^2 is a normalizing factor which might be different for each direction.

[41] Some of the mathematical techniques used in these programs have been discussed in an earlier paper (Ref. 34). The programs themselves are available from the Quantum Chemistry Program Exchange, Chemistry Department, Indiana University, Bloomington, Indiana.

[42] We include in these diagrams the tensor factors of the matrix elements.

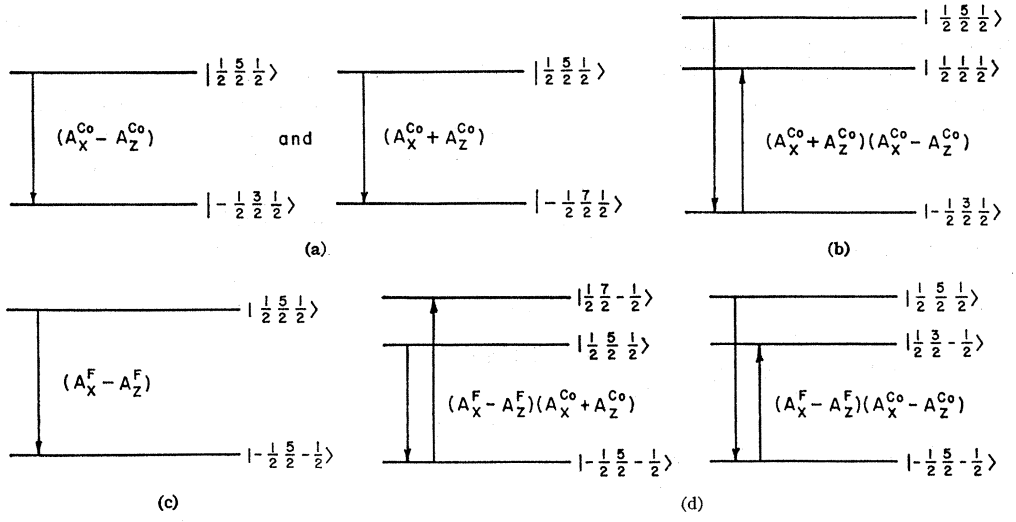

FIG. 8. Hyperfine perturbations for CoF.

Fig. 8(c), is small compared with the mutual fluorine-cobalt-spin corrections, Fig. 8(d). The first of these contributions is very large because it involves a particularly small energy denominator. There are no second-order corrections involving the fluorine hyperfine interaction only. The final terms indicated in Eq. (8) indicate that fourth-order corrections to the wave function are not negligible[43]; the first is proportional to $(A_x^{Co}-A_z^{Co})^2(A_x^{Co}+A_z^{Co})^2$ and the second to $(A_x^{F}-A_z^{F})(A_x^{Co}-A_z^{Co})^2(A_x^{Co}+A_z^{Co})$. The corrections corresponding to the mechanisms above are roughly 31, 23, 15, 15, 14, and 13 Mc/sec, respectively. The first three contributions correspond to the uneven spacings illustrated in Fig. 4. The fourth interaction affects all the fluoride spacings uniformly. The final interactions, whose magnitudes vary with the cobalt spin number, provide mechanisms for the observed variation of the effective fluorine splittings across the spectrum. Of course, since the mixings are very large in the function cited, perturbation estimates of the energy corrections are inaccurate, but they do indicate that large fourth-order corrections must be anticipated.

The generalization of the model problem to the complete Hamiltonian, Eq. (1), is most easily seen if the model Hamiltonian [Eq. (3)] is broken up differently for perturbation theory. Take as the zero-order Hamiltonian

$$\mathcal{H}_0^M=\mathbf{S}\times\mathbf{g}\times\mathbf{H}+\mathbf{S}\times\mathbf{A}^{Co}\times\mathbf{I}^{Co}+S_zA_z^{F}I_z^{F} \quad (9a)$$

and as the perturbation term

$$\mathcal{H}_1^M=S_xA_x^{F}I_x^{F}+S_yA_y^{F}I_y^{F}. \quad (9b)$$

To avoid degenerate perturbation theory the diagonal part of the fluorine hyperfine tensor is included in the zero-order Hamiltonian. Then, provided that the eigenstates of (9a) are not too close in energy to each other, the energy corrections induced by (9b) may be estimated in second-order perturbation theory. The most important modifications to the wave functions are small first-order corrections from states which conserve $(M_{Co}+M_F)$. These are schematically indicated in the upper part of Fig. 9, which is drawn to scale for the magnetic field in the y-direction. For $M_{Co}\leq\frac{3}{2}$, the perturbations *decrease* the observed shfs spacing; the effect becomes larger as M_{Co} progresses from $-\frac{7}{2}$ to $\frac{3}{2}$, because the zero-order states come closer to each other. However, since the $|\frac{1}{2}\,\frac{7}{2}\,-\frac{1}{2}\rangle$ state lies below the $|\frac{1}{2}\,\frac{5}{2}\,\frac{1}{2}\rangle$ state, here the perturbations *increase* the observed spacing.

The hypothetical fragment CoF_2 has the Hamiltonian [Eq. (9)] augmented by the hyperfine interaction of a second fluorine ion. If this ion is equivalent to the first, the first-order levels and the largest second-order perturbations take the form indicated in the lower

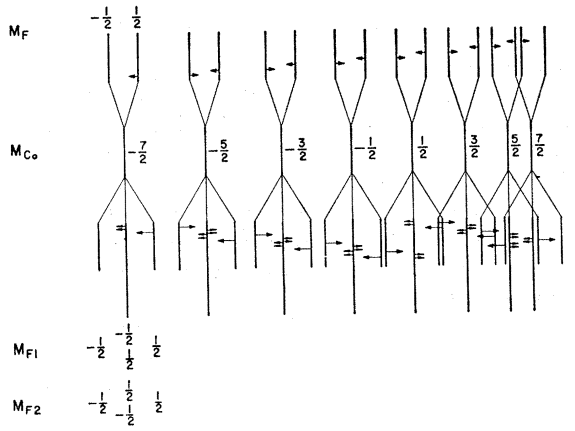

FIG. 9. Schematic indication of the largest second-order perturbations from the off-diagonal parts of the fluorine hyperfine interaction. In the upper portion the interactions are indicated for a hypothetical CoF fragment; in the lower, for a CoF_2 fragment. (The lengths of the arrows showing the perturbations do *not* indicate the magnitudes of the shifts.) The connected states are indicated by arrows at the same horizontal level.

[43] Note that nth-order corrections to the wave function are associated with $(2n)$th-order corrections to the energy.

portion of Fig. 9. If all the perturbations are small enough, so that no large changes in the eigenvectors are induced, the effective F^{19} hyperfine interaction for CoF approximates that for CoF_2 as follows. Denote the states for CoF_2 in an uncoupled representation $|M_S M_{Co} M_{F1} M_{F2}\rangle$,[44] and consider, for example, the states with $M_{Co}=-\frac{5}{2}$. Then $|\frac{1}{2}-\frac{5}{2}-\frac{1}{2}-\frac{1}{2}\rangle$ is perturbed both by $|\frac{1}{2}-\frac{7}{2}\frac{1}{2}-\frac{1}{2}\rangle$ and by $|\frac{1}{2}-\frac{7}{2}-\frac{1}{2}\frac{1}{2}\rangle$ by the same amount as $|\frac{1}{2}-\frac{5}{2}-\frac{1}{2}\rangle$ is perturbed by $|\frac{1}{2}-\frac{7}{2}\frac{1}{2}\rangle$ because the energy denominators as well as the matrix elements are the same for CoF_2 as for CoF. Also, since both $|\frac{1}{2}-\frac{5}{2}-\frac{1}{2}\frac{1}{2}\rangle$ and $|\frac{1}{2}-\frac{5}{2}\frac{1}{2}-\frac{1}{2}\rangle$ suffer the same perturbation from $|\frac{1}{2}-\frac{7}{2}\frac{1}{2}\frac{1}{2}\rangle$, their degeneracy is not split, but the levels are shifted only half as far as $|\frac{1}{2}-\frac{5}{2}-\frac{1}{2}-\frac{1}{2}\rangle$. So the perturbations do not disturb either statistical intensities or the relative spacings in the group of lines for any M_{Co}, but the hyperfine spacing changes from the first-order perturbation prediction. All the perturbations indicated in Fig. 9, and the smaller ones not indicated, are additive. Therefore, to a good approximation, fluorine hyperfine separations calculated by diagonalizing the 32×32 Hamiltonian for CoF may be transferred to the spectrum of CoF_2, and, by the same argument, to the Hamiltonian [Eq. (1)] for $(CoF_6)^{4-}$.

[44] In this paragraph, eigenkets with three quantum numbers belong to the CoF problem; those with four quantum numbers to the CoF_2 problem.

PHYSICAL REVIEW VOLUME 143, NUMBER 1 MARCH 1966

Approximation Methods in Many-Body Perturbation Theory*

BIRGER STÖLAN† AND LEON N. COOPER‡
Brown University, Providence, Rhode Island
(Received 17 June 1965)

An analysis of some approximations common in the treatment of many-body systems indicates that the inclusion of large numbers of uncancelled exclusion-principle-violating (EPV) processes leads to meaningless results. We therefore propose as a criterion for the validity of many-body approximations that there should be no such large-scale inclusion of EPV processes. The graphs generated in the BCS theory are analyzed from this point of view.

INTRODUCTION

In a recent paper, Fukushima and Fukuda[1] attempt to calculate the ground state of the BCS (Bardeen, Cooper, Schrieffer) reduced Hamiltonian in the strong-coupling limit by summing a subset of the totality of graphs generated by this Hamiltonian. The graphs chosen—ladder graphs—seem to dominate all others since they are of order Ω^0 whereas the neglected graphs are of order Ω^{-1} or lower. (The volume of the system is Ω.) As the ground-state energy of this system is known, it is possible to determine that the accuracy of their result is very poor and, what is worse, the asymptotic behavior of such functions as the vacuum expectation value of the U matrix is entirely incorrect. Since the subset of connected graphs chosen is a common one, and since its choice in their case seems particularly well justified, it seemed worthwhile to attempt to seek out the source of the difficulty. We state our conclusions in the language of the strong-coupling model although some are valid in general.

In the first part we summarize and analyze some of the results of Fukushima and Fukuda. This leads us to propose in Part II a criterion for the validity of many-body approximations. The third part contains an analysis of the BCS reduced Hamiltonian according to the proposed criterion.

I. THE LADDER APPROXIMATION

In the strong-coupling limit the kinetic-energy operator is replaced by its constant expectation value T. For convenience this constant is set equal to zero by a shift in the zero of the energy. The BCS reduced Hamiltonian in this limit is then

$$H=T+H_1=V\sum_{kk'}c_{k\uparrow}{}^{\dagger}c_{-k\downarrow}{}^{\dagger}C_{-k'\downarrow}C_{k'\uparrow}, \qquad (1.1)$$

where the sums over momenta are limited to a narrow shell around the Fermi surface. One of the authors has analyzed such strongly coupled systems for a general interaction[2]; some of the results are given below for reference.

The vacuum expectation value of the resolvent operator $R(z)$, where z is a complex variable, can be

* Supported in part by the Advanced Research Projects Agency, the National Science Foundation, and the U. S. Atomic Energy Commission.
† Present address: Physics Department, Norwegian Institute of Technology, Trondheim, Norway.
‡ Alfred P. Sloan Research Fellow.
[1] K. Fukushima and N. Fukuda, Progr. Theoret. Phys. (Kyoto) 28, 809 (1962).

[2] L. N. Cooper, Phys. Rev. 122, 1021 (1961).